

Robust LMI-Based Control of Wind Turbines with Parametric Uncertainties

Christoffer Sloth, Thomas Esbensen, Michael O.K. Niss, Jakob Stoustrup, and Peter F. Odgaard

Abstract—This paper considers the design of robust LMI-based controllers for a wind turbine along its entire nominal operating trajectory. The proposed robust controller design takes into account parametric uncertainties in the model using a structured uncertainty description, which makes the controllers less conservative than controllers designed using unstructured uncertainty descriptions. The LMI-based approach enables additional constraints to be included in the design, which is exploited to include requirements for minimizing fatigue loads and actuator usage.

Two different methods are adopted, of which the first method assumes full state information and therefore requires a separate observer. In contrast, the second method relies only on output feedback, but introduces complications in the design procedure in order to achieve feasibility in the solution of the control law.

Simulation results are obtained that show improved performance of the robust controllers in a comparison with a controller designed based on classical methods.

I. INTRODUCTION

Today, wind energy is the most competitive form of renewable energy. In the past decade the size and capacity of wind turbines have increased dramatically. Meanwhile, the structural components have been made relatively lighter to keep down costs. This has put higher demands on wind turbine control schemes, and implementation of advanced control systems is considered a promising way of decreasing fatigue loads.

In this paper a three-bladed horizontal-axis variable-speed variable-pitch wind turbine is considered, which works from the principle that wind acts on the blades making the rotor shaft rotate. The aerodynamic properties of the wind turbine are affected by the pitch angle of the blades, the speed of the rotor, and the effective wind speed. On this basis, an aerodynamic torque is applied to the rotor and the tower is affected by an aerodynamic thrust. The aerodynamic torque is transferred to the generator through a drive train in order to upscale the rotational speed of the rotor.

In terms of control, the wind turbine works in two distinct regions. Below a certain wind speed, in the partial load region, the turbine is controlled to generate as much power as possible. In the full load region, the wind turbine is controlled to produce a rated power output.

The traditional approach to wind turbine control is to apply gain-scheduling between a large number of classical

controllers, which are designed to be in the proximity of a certain operating point [1]. A large number of controllers may introduce instability issues due to extensive switching between the controllers, which of course must be avoided.

Various control approaches have been applied in relation to wind turbine control, such as LQ control [2], where state feedback is calculated based on a linearized plant model at a selected operating point. Additionally, MPC has been applied to include operational constraints in the design phase [3], while [4] considers LPV controllers that cover the entire nominal operating trajectory, but does not build upon a robust design method. Robust control synthesis options have been studied in [5] and [6], where uncertainties are represented using sensitivity functions. Both LPV and robust controllers take parameter variations into account, but in contrast to LPV controllers, robust controllers use constant control laws.

In this paper a robust controller design is presented, which covers the entire nominal operating trajectory and takes into account requirements that are met in today's operation of wind turbines. Parameter uncertainties of the aerodynamics are accounted for in the design, and robustness provides guaranteed stability and performance against these variations.

The proposed robust controller design separates from the previous referred robust designs by using a structured uncertainty description, which generally makes the controllers less conservative than controllers designed using unstructured uncertainty descriptions. This makes it possible to control the wind turbine along the entire nominal operating trajectory using fewer controllers than ordinary robust design methods, while maintaining the required performance.

Two LMI-based methods from [7] and [8] were adopted by this paper. The first method assumes full state information and therefore requires a separate observer to be designed (with challenges involved due to the lack of a robust separation theorem), whereas the second method is based on output feedback. One advantage of LMI-based methods is that additional constraints can be directly inserted, which makes the description adoptable to new constraints.

This paper is organized as follows. Section II describes the model of the wind turbine. In Section III a reference controller based on classical methods is presented to establish a frame of reference for the designed robust controllers. Section IV presents two different LMI-based methods for designing robust controllers taking parametric uncertainties into account. In Section V simulation results are presented, which compare the performance of the robust controllers to that of the reference controller. The paper is finalized by a conclusion in Section VI.

Christoffer Sloth, Thomas Esbensen, and Michael O.K. Niss are M.Sc. students at Automation and Control, Department of Electronic Systems, Aalborg University, Fredrik Bajers Vej 7C, DK-9220 Aalborg East, Denmark

Jakob Stoustrup is with Automation and Control, Department of Electronic Systems, Aalborg University, DK-9220 Aalborg East, Denmark

Peter F. Odgaard is with kk-electronic a/s, DK-8260 Viby J, Denmark

II. WIND TURBINE MODEL

A non-linear model of a wind turbine acts as a simulation model for the proposed control algorithms. The model is based on a static model of the aerodynamics, a two-mass model of the drive train, an electromechanical model of the generator, actuator models, and zero-mean Gaussian distributed measurement noises.

A. Aerodynamic Model

The rotor of the wind turbine converts energy from the wind to the rotor shaft, rotating at the speed $\omega_r(t)$. The power from the wind depends on the wind speed, the air density, ρ , and the swept area, A . From the available power in the swept area, the power on the rotor is given based on the power coefficient, $C_p(\lambda(t), \beta(t))$, which depends on the pitch angle of the blades, $\beta(t)$, and the ratio between the speed of the blade tip and the wind speed, denoted tip-speed ratio, $\lambda(t)$. The aerodynamic torque applied to the rotor by the effective wind speed passing through the rotor, $v_r(t)$, is given as:

$$T_a(t) = \frac{1}{2\omega_r(t)} \rho A v_r^3(t) C_p(\lambda(t), \beta(t)) \quad [\text{Nm}] \quad (1)$$

The coefficient C_p describes the aerodynamic efficiency of the rotor by a nonlinear mapping as illustrated in Fig. 1.

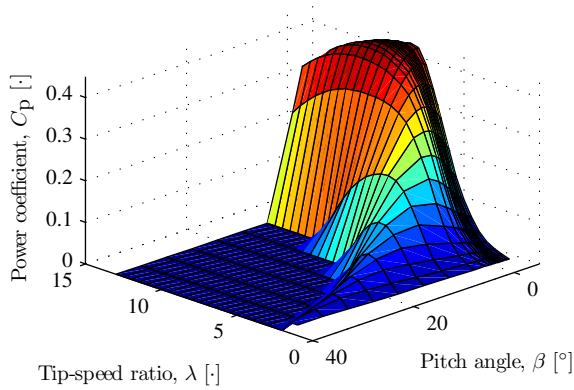


Fig. 1. Illustration of the power coefficient, C_p .

B. Drive Train Model

The drive train model consists of a low-speed shaft and a high-speed shaft having inertias J_r and J_g . The shafts are interconnected by a gear ratio, N_g , combined with torsion stiffness, K_{dt} , and torsion damping, B_{dt} , which result in a torsion angle $\theta_{\Delta}(t)$. The drive train has efficiency η_{dt} and drives the loading torque from the generator, $T_g(t)$, at a speed $\omega_g(t)$. The linear model is given as:

$$J_r \dot{\omega}_r(t) = T_a(t) - K_{dt} \theta_{\Delta}(t) - B_{dt} \dot{\theta}_{\Delta}(t) \quad [\text{Nm}] \quad (2)$$

$$J_g \dot{\omega}_g(t) = \frac{\eta_{dt} K_{dt}}{N_g} \theta_{\Delta}(t) + \frac{\eta_{dt} B_{dt}}{N_g} \dot{\theta}_{\Delta}(t) - T_g(t) \quad [\text{Nm}] \quad (3)$$

$$\dot{\theta}_{\Delta}(t) = \omega_r(t) - \frac{1}{N_g} \omega_g(t) \quad [\text{rad/s}] \quad (4)$$

C. Pitch System Model

The pitch system tracks a reference, $\beta_{ref}(t)$, and is modeled as a first order system. Its time constant is τ , and includes also a communication delay, t_d .

$$\dot{\beta}(t) = -\frac{1}{\tau} \beta(t) + \frac{1}{\tau} \beta_{ref}(t - t_d) \quad [^\circ/\text{s}] \quad (5)$$

Besides the linear dynamics described by (5), the model also includes constraints on the slew rate and operational range.

D. Generator and Converter Models

Electric power is generated by the generator, while a power converter interfaces the wind turbine generator output with the utility grid and controls the currents in the generator. The generator torque in (6) is adjusted by the reference $T_{g,ref}(t)$. The dynamics of the converter is approximated by a first order system with time constant τ_g and communication delay $t_{g,d}$. Just as for the model of the pitch system, the slew rate and operational range of the converter are limited.

$$\dot{T}_g(t) = -\frac{1}{\tau_g} T_g(t) + \frac{1}{\tau_g} T_{g,ref}(t - t_{g,d}) \quad [\text{Nm/s}] \quad (6)$$

The power produced by the generator can be approximated from the mechanical power calculated below, where η_g denotes the efficiency of the generator, which is assumed constant.

$$P_g(t) = \eta_g \omega_g(t) T_g(t) \quad [\text{W}] \quad (7)$$

E. Assembled Model

The interconnection of the wind turbine sub-models is illustrated in Fig. 2. The input to the model is provided by a modified version of the wind model SB-2 in [9], to which the swaying of the tower is added.

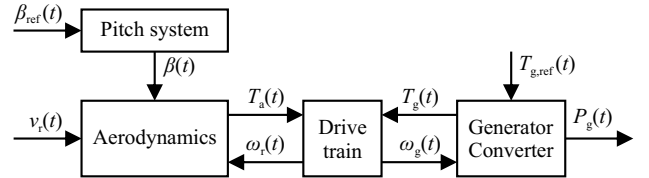


Fig. 2. Block diagram of the wind turbine model.

Available measurements are: generator torque, pitch angle, generator speed, and rotor speed; all sampled at a rate of 100 Hz. The output power is not available as an actual measurement, but is evaluated as the product of the measurements of the generator speed and generator torque. To present the quality of the measurements, these are emulated as deterministic values with addition of zero-mean Gaussian noises with the following standard deviations: $\sigma_{T_g} = 90$ Nm, $\sigma_{\beta} = 0.2^\circ$, $\sigma_{\omega_g} = 0.05$ rad/s, and $\sigma_{\omega_r} = 0.025$ rad/s.

F. Model Parameters

The following parameters are chosen such that they represent a realistic but fictitious turbine: $A = 10,387$ m², $\rho = 1.225$ kg/m³, $B_{dt} = 9.45$ MNm/(rad/s), $J_r = 55 \cdot 10^6$ kgm², $J_g = 390$ kgm², $K_{dt} = 2.7$ GNm/rad, $N_g = 95$, $\eta_{dt} = 0.97$, $t_d = 10$ ms, $\tau = 50$ ms, $t_{g,d} = 20$ ms, $\tau_g = 10$ ms, $\eta_g = 0.92$.

III. REFERENCE CONTROLLER

The purpose of the reference controller is to enable performance comparison of the robust controllers with a controller, which is designed using classical principles and corresponds to a simplified wind turbine controller.

In partial load operation the controller should maximize the power output of the wind turbine by tracking the maximum of the C_p -surface, $C_{p,\max}$ at λ_{opt} . This was accomplished by applying a generator torque that maximizes the power output in steady-state, as in [10]. This is based on (1) and is shown below.

$$T_g(t) = \frac{1}{2} \rho A \frac{\eta_{\text{dt}} R^3}{N_g^3 \lambda_{\text{opt}}^3} C_{p,\max} \omega_g^2(t) \quad [\text{Nm}] \quad (8)$$

In full load operation two PI-controllers were used to track constant generator speed and output power references: a speed controller controls the pitch angle of the blades while a power controller controls the generator torque. Both controllers can be expressed on this general form:

$$D(s) = K \left(1 + \frac{1}{T_i \cdot s} \right) \quad (9)$$

The speed controller consisted of two controllers operating at wind speeds of 12-15 m/s and 15-25 m/s respectively. The controller parameters are:

$$\begin{aligned} \text{Speed Controller 1:} & \quad K = 8^\circ/(\text{rad/s}), T_i = 8 \text{ s} \\ \text{Speed Controller 2:} & \quad K = 4^\circ/(\text{rad/s}), T_i = 4 \text{ s} \\ \text{Power Controller:} & \quad K = 0.0067 \text{ Nm/W}, T_i = 0.15 \text{ s} \end{aligned}$$

IV. CONTROLLER DESIGN

This section presents two different LMI-based methods for designing a robust controller taking parametric uncertainties into account. The wind turbine model has parametric uncertainties, as it relies on the C_p -surface. This introduces three partial derivatives in the system description, which all depend on the point of operation. The robust design methods handle the uncertainties and provide both stability and performance guarantees.

The two methods were chosen as they are based on a structured uncertainty description, which makes the controllers less conservative than an unstructured uncertainty description, making this description favorable. In both methods the uncertainties in the system are assumed to be polytopic. This means that the system having varying parameters can be expressed as:

$$\dot{x}(t) = A_\Delta x(t) + B_{1\Delta} w(t) + B_{2\Delta} u(t) \quad (10a)$$

$$z(t) = C_{1\Delta} x(t) + D_{11\Delta} w(t) + D_{12\Delta} u(t) \quad (10b)$$

$$y(t) = C_{2\Delta} x(t) + D_{21\Delta} w(t) \quad (10c)$$

The matrices of the uncertain system must be represented as polytopic functions of the uncertain parameters, Δ , as

shown below, to be able to utilize the design methods.

$$\begin{bmatrix} A_\Delta & B_{1\Delta} & B_{2\Delta} \\ C_{1\Delta} & D_{11\Delta} & D_{12\Delta} \\ C_{2\Delta} & D_{21\Delta} & 0 \end{bmatrix} = \begin{bmatrix} A & B_1 & B_2 \\ C_1 & D_{11} & D_{12} \\ C_2 & D_{21} & 0 \end{bmatrix} + \begin{bmatrix} B_0 \\ D_{10} \\ D_{20} \end{bmatrix} \Delta [C_0 \quad D_{01} \quad D_{02}] \quad (11)$$

In the uncertainty description, the dimension of Δ should be as low as possible to decrease the size of the uncertainty space, since a larger uncertainty space results in a more conservative controller.

The first method assumes full state information and therefore requires a separate observer to be designed, introducing some challenges due to the lack of a robust separation theorem. Conversely, the second method relies on the measured variables, eliminating the issue of the first method. The different assumptions have some consequences for the solvability of the LMIs used in the controller designs. The search for a solution to the LMIs in the first method is convex, while the search is non-convex in the second method making it necessary to solve these LMIs in two steps. The optimization problems were set up in YALMIP and solved with SeDuMi, based on balanced state-space realizations.

In order to achieve the objectives of wind turbine control, additional constraints were introduced in the LMIs. As performance criteria, the design must maximize the efficiency of the wind turbine at partial load and minimize power fluctuations and variations in generator speed at full load. Furthermore, fatigue loads in the drive train must be minimized with minimal actuator usage.

A. Robust State Feedback Control

In [7] a robust state feedback design method is described based on a structured uncertainty description. This method was used to calculate a full state feedback control law. This implied that an observer had to be designed, since full state information was not available. The observer utilized to provide full state information was an optimal observer, but this will not be described in this paper. It should be noted that, as there is no general separation theorem for robust controllers, the actual robustness obtained by this approach will have to be evaluated by a subsequent analysis. Due to space limitations, we have not included this analysis.

The LMI that must be solved in order to obtain a robust state feedback controller is shown below, where $R_\Delta = I - D_{11\Delta}^T D_{11\Delta}$. Notice that '*' is inferred by symmetry and that the bold symbols are unknown matrices.

$$\begin{bmatrix} A_\Delta \mathbf{X} + B_{2\Delta} \mathbf{W} + (*) & * & * \\ B_{1\Delta}^T + D_{11\Delta}^T C_{1\Delta} \mathbf{X} + D_{11\Delta}^T D_{12\Delta} \mathbf{W} & -R_\Delta & * \\ C_{1\Delta} \mathbf{X} + D_{12\Delta} \mathbf{W} & 0 & -I \end{bmatrix} \prec 0 \quad (12)$$

The solution of this LMI is a convex search for a matrix \mathbf{W} and a matrix $\mathbf{X} = \mathbf{X}^T \succ 0$. The LMI must be satisfied for all $\Delta \in \Delta_{\text{vex}}$, where Δ_{vex} denotes the vertex points of Δ .

After finding X and W the state feedback controller for the control law $u(t) = Fx(t)$ can be calculated as shown below.

$$F = WX^{-1} \quad (13)$$

B. Robust Output Feedback Control

In [8] a method for designing a robust output feedback controller is proposed. This method also relies on a structured uncertainty description, but uses output feedback. Therefore, both methods share an identical uncertainty description. In [8] a two-step design procedure is proposed, where under certain constraints the search in the second step is guaranteed to be feasible.

The purpose of this design method is to calculate a robust dynamic output feedback controller on the following form:

$$\dot{x}_c(t) = A_c x_c(t) + B_c y(t) \quad (14a)$$

$$u(t) = C_c x_c(t) \quad (14b)$$

The BMI description which must be solved to obtain robust output feedback are shown below, where $A_\Delta = A + \Delta A$ etc.

$$\begin{bmatrix} Y & I \\ I & X \end{bmatrix} \succ 0 \quad (15)$$

$$\begin{bmatrix} \phi_{11} & * & * & * \\ \phi_{12}^T & \phi_{22} & * & * \\ C_1 & C_1 X + D_{12} W_c & -\gamma I & * \\ B_1^T Y + D_{21}^T W_o^T & B_1^T & D_{11}^T & -\gamma I \end{bmatrix} \prec 0 \quad (16)$$

$$\phi_{11} = Y(A + \Delta A) + W_o(C_2 + \Delta C_2) + (*)$$

$$\phi_{12} = L + Y\Delta A X + Y\Delta B_2 W_c + W_o\Delta C_2 X + \Delta A^T$$

$$\phi_{22} = (A + \Delta A)X + (B_2 + \Delta B_2)W_c + (*)$$

When the BMI description is solved, the controller can be synthesized using:

$$A_c = -(Y - X^{-1})^{-1} (L - YAX - YB_2 W_c - W_o C_2 X - A^T) X^{-1} \quad (17)$$

$$B_c = -(Y - X^{-1})^{-1} W_o, \quad C_c = W_c X^{-1} \quad (18)$$

The search for the unknown variables is not convex due to the term ϕ_{12} , where two unknown quantities are multiplied. Therefore, a two-step procedure, based on solving LMIs, is proposed using the two necessary conditions shown below.

$$\begin{bmatrix} (A + \Delta A)X + (B_2 + \Delta B_2)W_c + (*) & * & * \\ C_1 X + D_{12} W_c & -\gamma I & * \\ B_1^T & D_{11}^T & -\gamma I \end{bmatrix} \prec 0 \quad (19)$$

$$\begin{bmatrix} Y(A + \Delta A) + W_o(C_2 + \Delta C_2) + (*) & * & * \\ C_1 & -\gamma I & * \\ B_1^T Y + D_{21}^T W_o^T & D_{11}^T & -\gamma I \end{bmatrix} \prec 0 \quad (20)$$

The idea is to find a solution to the non-convex problem by finding a feasible point in one of the necessary conditions, (19) or (20), which should be inserted into (16).

If it is chosen to solve (19), the convex search for the remaining variables, Y , W_o , and L is guaranteed only if

$\Delta C_2 = 0$ and $(A, [B_1, B_0, B_o], C_2, [D_{21} \ 0 \ 0])$ are both left invertible and minimum phase.

To test if the system is left invertible the following equation is utilized, where $u \in \mathbb{R}^m$:

$$\text{rank} \left(C (sI - A)^{-1} B \right) = m \quad (21)$$

The above equation shows that the number of measurements must be greater than or equal to the number of disturbance inputs to the system plus the number of uncertain parameters. This condition is not satisfied in the considered wind turbine control system; hence, the second search is not guaranteed to be feasible. Therefore, it is difficult to use the two-step procedure, since the unknown parameters found in the first search are included in the second search. The approach utilized in the non-convex design, for the partial load region, was to compute a feasible point for (19) and (20) in the first search, to determine the one that was hardest to fulfill. In this case (20) was the hardest to fulfill, since this LMI was very sensitive to the measurement noise, as the matrix D_{21} appears only in (20).

C. Controller Design

Before designing controllers using the two methods described above, it was decided to design an effective wind speed estimator for both setups. This was chosen, since only a measurement of a point wind speed is usually available.

Wind Speed Estimator: The wind speed estimator was based on a design proposed in [11], where the aerodynamic torque is estimated using a PI-controller having the error of the estimated generator speed as input. This torque is combined with the pitch angle and rotor speed to calculate the wind speed.

By rewriting (1) the C_p -value and tip-speed ratio can be isolated as shown below.

$$\frac{2T_a(t)}{\rho \pi R^5 \omega_r^2(t)} = \frac{C_p(\lambda(t), \beta(t))}{\lambda^3(t)} \quad [\cdot] \quad (22)$$

The left hand side of the equation consists of known quantities, while the right hand side is dependent on the unknown wind speed. The right hand side can be reformulated into a new lookup table, which then gives the tip-speed ratio. From this value the wind speed can be estimated using $\omega_r(t)$.

The remaining controller design for the wind turbine consists of two separate parts; designing an uncertainty model and setting up a performance specification, which can be included in the LMIs.

Uncertainty Model: It was assumed that the main uncertain part of the model is caused by the non-linear nature of the aerodynamics. The instantaneous partial derivatives of the aerodynamic torque are part of the linearized model; hence, these were described in an uncertain manner.

It was discovered by plotting the partial derivatives of the aerodynamic torque, along the nominal operating trajectory, that these are all approximately affine functions of the wind speed, when divided into four regions. This made it possible to describe the uncertainties using only one uncertain parameter, i.e. $\Delta = v_r$.

The designed system was divided into four regions, denoted Region 1, Region 2 etc., for three reasons: minimize the magnitude of the uncertain parameter to maximize performance in the considered region, justify the affine approximation of the uncertain parameters, and minimize the number of regions to avoid extensive switching. To illustrate this division, the partial derivative of $T_a(t)$ with respect to ω_r along the operating trajectory is shown in Fig. 3.

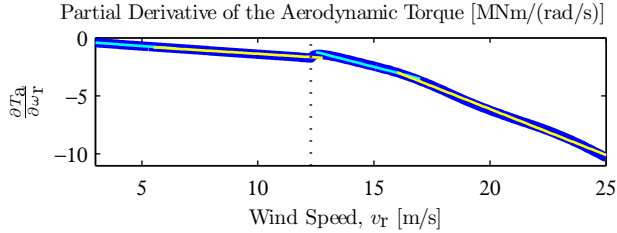


Fig. 3. Partial derivative of $T_a(t)$ with respect to ω_r along the nominal operating trajectory. The vertical dotted line represents the rated wind speed, while the overlapping straight lines are affine approximations in the four regions.

Introduction of multiple regions creates an additional design challenge, as bumpless transfer has to be designed. The method used was based on a Youla-Kucera parameterization, and is described in [12] for the considered system.

Performance Specification: In both of the presented methods, the performance specification provided the opportunity for tuning the controllers. The specification was based on a mixed sensitivity description, where it was chosen to specify sensitivity and control sensitivity. This type of description makes it possible to specify performance requirements in the frequency domain.

The mixed sensitivity description was implemented as shown in Fig. 4, where $W_S(s)$ is the sensitivity filter and $W_M(s)$ is the control sensitivity filter.

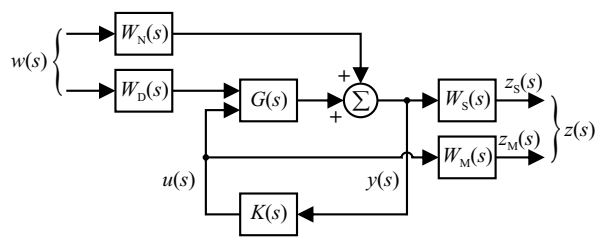


Fig. 4. Block diagram of the mixed sensitivity description.

In addition to the sensitivity filters, the input disturbance filter, $W_D(s)$, and the filter adding measurement noise to the measurements, $W_N(s)$, were also added to the description.

The performance measures are $z(t)$, and the vector going to the mixed sensitivity filters is denoted $\xi(t)$. The specification specified the maximum tracking errors, the integral of these, and the actuator usage, as shown in the vector below.

$$\xi(t) = \begin{bmatrix} \omega_{g,e}(t) & P_{g,e}(t) & \int \omega_{g,e}(t) dt & \int P_{g,e}(t) dt & \dot{\beta}(t) \\ T_{g,\text{ref}}(t) & \beta_{\text{ref}}(t) \end{bmatrix}^T \quad (23)$$

In the design of the controllers the performance vector, $\xi(t)$, became part of the state vector of the system; hence, it was used in the feedback controllers, but in the implementation this part of the system became part of the controllers and was implemented using the ordinary state vector of the system.

V. SIMULATION RESULTS

Simulations were performed in MATLAB Simulink using the non-linear model provided in Section II. In this section two different simulations are presented, since the robust output feedback controller was implemented for partial load operation only.

The first simulation compares the performance of the reference controller and robust state feedback controller at wind speeds covering the entire operating range of the wind turbine. The second simulation compares the performance of the reference controller, robust state feedback controller, and robust output feedback controller at partial load operation.

The performance of the controllers was compared by calculating the actuator usage, drive train stress, and produced power.

Evaluation of the Robust State Feedback Controller

A simulation was performed for the robust state feedback controller, where the wind turbine operated in both partial and full load operation. The mean wind speed signal used in the simulations was a measurement from a real wind turbine. The duration of the simulation was 3,540 s, from which a sequence of 60 s is plotted in Fig. 5.

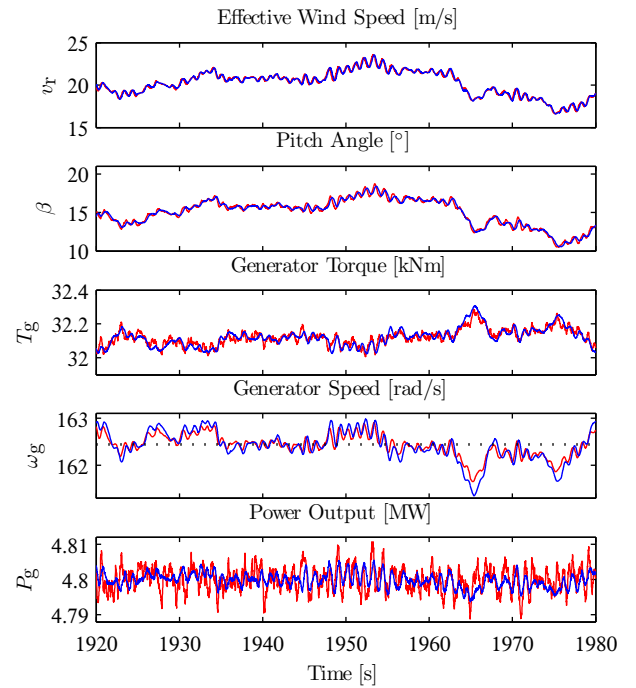


Fig. 5. Simulation result of the reference controller (red) and the robust state feedback controller (blue).

From the figure it is clear that the output power and the usage of the generator torque were less fluctuating for

the robust state feedback controller than for the reference controller. The performance measures for the wind turbine are set up in Table I, where the results are normalized to the performance of the reference controller.

TABLE I

Evaluated performance measures for partial and full load operation.

Partial Load Operation		
	Reference	Robust
$\int \hat{\theta}_{\Delta}^2(t)dt$	1.00	0.95
$-\int P_g(t)dt$	1.00	1.00
$\int \dot{T}_g(t) dt$	1.00	1.59
Full Load Operation		
	Reference	Robust
$\int \hat{\theta}_{\Delta}^2(t)dt$	1.00	0.88
$\int (P_{g,N} - P_g(t))^2 dt$	1.00	0.43
$\max(P_{g,N} - P_g(t))$	1.00	0.77
$\int \dot{\beta}(t) dt$	1.00	0.82
$\int \dot{T}_g(t) dt$	1.00	0.63

The table shows that the performance of the two controllers was similar in partial load operation, but that the robust controller performed better in full load operation.

Evaluation of the Robust Output Feedback Controller

A simulation was performed for comparing the performance of the robust output feedback controller to the performance of both the robust state feedback controller and the reference controller. The wind turbine operated in partial load operation for 350 s.

The results of the simulation are shown in Table II, where Robust 1 denotes the robust state feedback controller and Robust 2 refers to the robust output feedback controller.

TABLE II

Evaluated performance measures in partial load operation for the three designed controllers.

	Reference	Robust 1	Robust 2
$\int \hat{\theta}_{\Delta}^2(t)dt$	1.00	0.93	0.49
$-\int P_g(t)dt$	1.00	1.00	1.00

The table shows that the power output using the three controllers was the same, but that the stress on the drive train was significantly decreased by the robust output feedback controller.

The results indicate that the robust controllers may lead to an improved control in the sense of minimizing the performance measures, since the robust design method takes the varying parameters into account.

VI. CONCLUSION

This paper addresses the design of LMI-based robust controllers to control a variable-speed variable-pitch wind turbine, while taking into account parametric uncertainties in the aerodynamic model. Two different methods are adopted,

of which the first method assumes full state information and therefore requires a separate observer to be designed, whereas the second method relies only on measured variables.

The performance of the robust state feedback controller is compared to that of a controller designed using classical methods. The comparison shows that the two controllers have similar performance in partial load operation, while the robust controller shows improved performance in terms of stress on the drive train and actuator usage in full load operation. The robust output feedback controller is compared to the other two controllers in partial load operation and shows improved performance in terms of stress on the drive train.

The disadvantages of the utilized methods are the lack of a robust separation theorem in the first method and the increased complexity in the design procedure in order to achieve feasibility in both methods. Especially the robust output feedback method introduces feasibility problems, since it is based on a two-step procedure, where no guarantees of feasibility necessarily exist for solving the second step.

In general, the advantage of the two design methods, compared to classical design methods, is that parameter variations can be included in the design procedure, providing stability and performance guarantees along the entire operating trajectory of the wind turbine system.

REFERENCES

- [1] K. Hammerum, "A fatigue approach to wind turbine control", *Master's Thesis*, Technical University of Denmark, 2006.
- [2] N.K. Poulsen, T.J. Larsen, and M.H. Hansen, "Comparison between a PI and LQ-regulation for a 2 MW wind turbine", *Tech. Rep.*, Risø National Laboratory, 2005.
- [3] L.C. Henriksen and N.K. Poulsen, "Model Predictive Control of a Wind Turbine with Constraints", In *Proceedings of EWEC 2008*, Brussels, Belgium, MAR 2008.
- [4] K.Z. Østergaard, J. Stoustrup, P. Brath, "Linear parameter varying control of wind turbines covering both partial load and full load conditions", *International Journal of Robust and Nonlinear Control*, 2008, pp. 92-116.
- [5] B. Connor, S.N. Iyer, W.E. Leithead, and M.J. Grimble, "Control of a horizontal axis wind turbine using H_{∞} control", In *Proceedings of the first IEEE Conference on Control Applications*, vol. 1, SEP 1992, pp. 117-122.
- [6] R. Rocha, L.S.M. Filho, and M.V. Bortolus, "Optimal Multivariable Control for Wind Energy Conversion System - A comparison between H_2 and H_{∞} controllers", In *Proceedings of the 44th IEEE Conference on Decision & Control*, DEC 2005, pp. 7906-7911.
- [7] K. Zhou, P.P. Khargonekar, J. Stoustrup, and H.H. Niemann, "Robust Performance of Systems with Structured Uncertainties in State Space", *Automatica*, vol. 31, no. 2, FEB 1995, pp. 249-255.
- [8] F. Jabbari, "Output Feedback Controllers for Systems with Structured Uncertainties", *IEEE Transactions on Automatic Control*, vol. 42, no. 5, MAY 1997, pp. 715-719.
- [9] Aalborg University and Risø National Laboratory, "Wind Turbine Blockset", 2005, http://www.iet.aau.dk/Research/research_prog/wind_turbine/Projects/SimPlatformPrj/.
- [10] K.E. Johnson, L.Y. Pao, M.J. Balas, and L.J. Fingersh, "Control of variable-speed wind turbines: standard and adaptive techniques for maximizing energy capture", *IEEE Control Systems Magazine*, JUN 2006, pp. 70-81.
- [11] K.Z. Østergaard, P. Brath, and J. Stoustrup, "Estimation of effective wind speed", *Journal of Physics: Conference Series*, vol. 75, 2007.
- [12] M.O.K. Niss, T. Esbensen, C. Sloth, J. Stoustrup, and P.F. Odgaard, "A Youla-Kucera approach to Gain-Scheduling with Application to Wind Turbine Control", In *Proceedings of the 3rd IEEE Multi-conference on Systems and Control*, Saint Petersburg, Russia, JUL 2009.